Applying Active Foil Bearings with Bimorph Piezoelectric Drives in Microturbines for Distributed Energy Systems

A. V. Sytin, D. V. Shutin(✉), and R. N. Polyakov

Oryol State University Named After I.S. Turgenev, 95, Komsomolskaya Street, Orel 302026, Russia
rover.ru@gmail.com

Abstract. The article considers the use of adaptive mechatronic bearings in high-speed microturbines of micro power plants for distributed energy systems. Thrust gas-dynamic bearings with an elastically pliable bearing surface, namely gas foil bearings, are considered. The authors propose using bimorph piezoelectric elements in multilayer foils operating in the generator mode to determine the foils deformation, as well as in the actuator mode to make the required parameters of the bearing surface. The technological process of its manufacturing is described. A mathematical model of such bearing based on the Reynolds equation for a gas lubricant layer, as well as the equation of the piezoelectric effect, is shown. The influence of construction parameters, such as materials and thicknesses of corresponding layers in a foil, has been studied. The simulation also shows changes in the frequency response characteristic of the rotor-bearing system with an active foil bearing. Changing the bearing stiffness by applying voltage to piezodrives in foils can result in reducing the amplitude of rotor vibrations if an appropriate algorithm of voltage changing is used.

Keywords: Bimorph piezoelectric drive · Foil bearing · Active control · Microturbines · Vibration · Frequency response

1 Introduction

Currently, one of main trends in energy generation and distribution is using small-generation plants as a regular source of reserve capacity. About 12 million small distributed generation units (unit capacity up to 60 MW) with a total capacity of over 220 GW operate in the USA. The growth rate is about 5 GW per year. In EU countries, distributed generation is about 10% of total electricity production (in Denmark-45%). The most promising is the process of cogeneration—the joint generation of electricity and heat using a single source of primary energy. Cogeneration is the most effective solution for reconstruction of boiler houses which are converted to gas mini power plants. Cogeneration is also modern and economically effective solution for power supply of office buildings, shopping centers, and sports facilities [1–3].

For a long time, from the 60 s to the 90 s of the twentieth century, there were limitations of distributed energy systems due to inadequate technologies. Some limitations were overcome during commercial production of a completely new class of power

A. A. Radionov and V. R. Gasiyarov (eds.), *Proceedings of the 6th International Conference on Industrial Engineering (ICIE 2020)*, Lecture Notes in Mechanical Engineering, https://doi.org/10.1007/978-3-030-54814-8_53

equipment—microturbines (15 kW–1 MW) and low-power radial turbines (2 MW). Now, some international companies produce rather reliable, simple, and relatively inexpensive gas small and microturbines [3]. Their main advantages are compactness, compliance with environmental requirements, low noise and vibration, the technical ability to change the load quickly without significant efficiency reducing, and good efficiency in cogeneration. [4–6].

2 Foil Bearings in Microturbines

Compared to large turbomachines, the low weight of microturbines' shafts reduces its inertia and provides faster response to changes in power load. The rotating speed of a microturbine's shaft can reach 100,000 rpm. Modern generators with permanent magnets can generate the output voltage about 280 V at such rotation frequency [7–10]. Such power characteristics allow using thin-walled bimorph piezoelectric drives for changing characteristics of foil air bearings.

The first foil bearing with such drives was designed in 1992 by Tsumaki Nobuo [11]. The piezoelectric elements operate in generator mode, based on the direct piezoelectric effect. Such design allows make a system for monitoring the operational condition of a foil bearing based on signals generated during the deformation of piezoelectric bimorph elements. Comparing these signals with permissible deformations of foils allows constant monitoring the state of the elastic surface and preventing failures in a rotor-bearing system. According to the NASA reports and various researches on foil gas-dynamic bearings, start and stop periods are most dangerous as there is direct contact and friction between the shaft and the foils. To ensure wear resistance of the surface of elastic piezoelectric elements, they must be covered with wear-resistant anti-friction coatings [12, 13].

In general case, a single elastic element of a foil bearing is a multilayer structure (Fig. 1a). The middle layers must contain an elastic base to provide the rigidity and fatigue strength of a bimorph piezoelectric element. Piezoceramic plates located on opposite surfaces of an elastic base must have a different connection sign, as shown in Fig. 1a. The top layer of the multilayer structure must be a layer of anti-friction wear-resistant material.

A single stage of assembling the described multilayer thrust foil gas-dynamic bearing with bimorph piezoelectric elements is shown in Fig. 1b. The central base of a composite foil can be made of copper, beryl bronze, stainless steel, or some other metal. The base plate increases the mechanical strength of the bimorph, but reduces displacement rate. The shown base for the composite foil is made of spring steel 65Mn. Protection of the foil's surface from corrosion and other damaging external factors was implemented by covering it with a special varnish, also providing electric insulation properties.

After installing the electrodes, the plate is polarized in a strong constant electric field and acquires piezoelectric properties. Multilayer technology increases flexibility and allows for increased actuator movement. At the last stage, the foil top surface is covered with anti-friction coating using conventional staining techniques (spraying, screen printing, dipping, brushing, etc.). After coating and drying, the solvent evaporates, and the binders polymerize and provide reliable adhesion to the substrate. The staining method

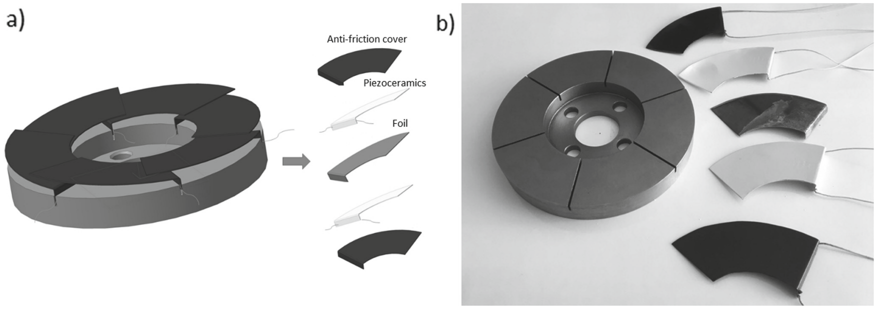

Fig. 1 **a** Scheme and **b** photo of a thrust foil gas-dynamic bearing with bimorph piezoelectric elements

is chosen depending on the geometry of the foils, required uniformity and durability of the coatings [14–16].

The resulting operational scheme of a multilayer foil of thickness h and length L with bimorph piezoelement is shown in Fig. 2. F is a force generated by a piezodrive under applied voltage U_{in}, and ΔX is maximal displacement of a free foil. Direction of force F and displacement ΔX depends on polarity of applied voltage U_{in}.

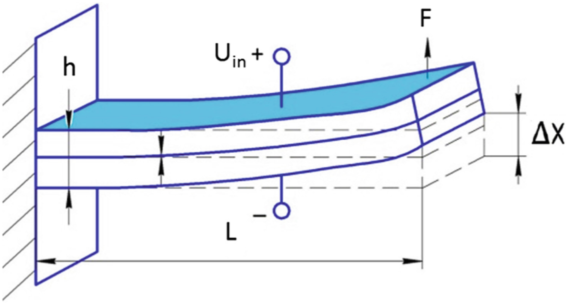

Fig. 2 Operational scheme of a multilayer foil with bimorph piezoelement

3 Modeling of Foil Bearings with Piezoelectric Drives

In order to design an appropriate configuration of the described foil bearing, its mathematical model has been developed. The model takes into account pressure distribution in a gas lubricant layer, elastic deformation of foils under this pressure and external forces, and also the piezoelectric effect [17, 18].The diagram of the modelled bearing is shown in Fig. 3.

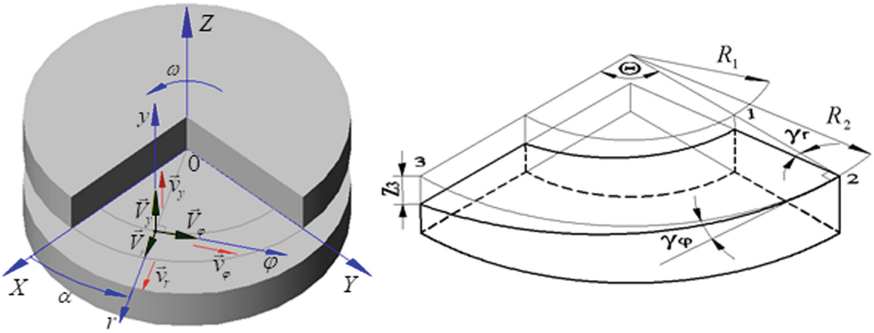

Fig. 3 Diagram of a thrust fluid-film bearing

Calculation of fluid-film bearings, including gas bearings, is based on determining a pressure field in a lubricant layer. The Reynolds equation for a gas bearing is [19]:

$$\frac{\partial}{r\partial r}\left[\frac{\rho r h^3}{\mu K_r}\frac{\partial p}{\partial r}\right]+\frac{\partial}{r\partial\varphi}\left[\frac{\rho h^3}{\mu K_\phi}\frac{\partial p}{r\partial\varphi}\right]=12h\frac{\partial\rho}{\partial t}+6\frac{\partial}{r\partial r}(\rho r h V_r)+6\frac{\partial}{r\partial\varphi}\left(\rho h V_\varphi\right)+12\rho V_y, \tag{1}$$

where $p = p(r, \varphi)$ is gas pressure, ρ is density, μ is viscosity, ω is angle speed, K_r and K_φ are the corresponding turbulence coefficients. Values of velocities of points on a bearing surface are as follow:

$$\begin{aligned} V_r &= \dot{X}\cos\alpha + \dot{Y}\sin\alpha; \\ V_\varphi &= \omega r + \dot{X}\sin\alpha - \dot{Y}\cos\alpha; \\ V_y &= \dot{Z}. \end{aligned} \tag{2}$$

The geometry of radial gap is described by a function that also is a part of the Reynolds Eq. (1):

$$\begin{cases} h(r,\varphi) = h_0 + h_k + w* \\ w* = w + w_{PE} \end{cases}, \tag{3}$$

where h_0 is initial gap, h_k is gap formed by an inclined surface of a foil, w is a value of a foil deflection under the lubricant pressure, w_{PE} is a value of a foil deflection due to reversed piezoelectric effect calculated as follow:

$$w_{\mathrm{PE}} = E\cdot d_{ij}\cdot l_0 \tag{4}$$

where l_0 is a piezoceramic plate thickness, E is strength of electric field, d_{ij} is piezomodule of piezoceramic material.

As the length and the width of a foil are much larger than its thickness, foil can be considered as thin plates [20]. Thereby, each foil of a thrust foil bearing can be calculated as a sector plate. Its deflection is described by the Germain–Lagrange differential equation that in cylindrical coordinates takes the form:

$$\left(\frac{\partial}{\partial r^2}+\frac{1}{r}\frac{\partial}{\partial r}+\frac{1}{r^2}\frac{\partial}{\partial\theta}\right)\left(\frac{\partial w}{\partial r^2}+\frac{1}{r}\frac{\partial w}{\partial r}+\frac{1}{r^2}\frac{\partial w}{\partial\theta}\right)=\frac{p}{D}, \tag{5}$$

where p is pressure on a plate, D is rigidity of a plate at bending, defined as:

$$D = \frac{Eh^3}{12(1 - \mu^2)}, \tag{6}$$

where h is a foil thickness, E is Young's modulus of the material of a foil, μ is Poisson's ratio of the material of the foil. By varying these parameters, it is possible to achieve different stiffness values of the foil and optimize the whole bearing characteristics [21, 22].

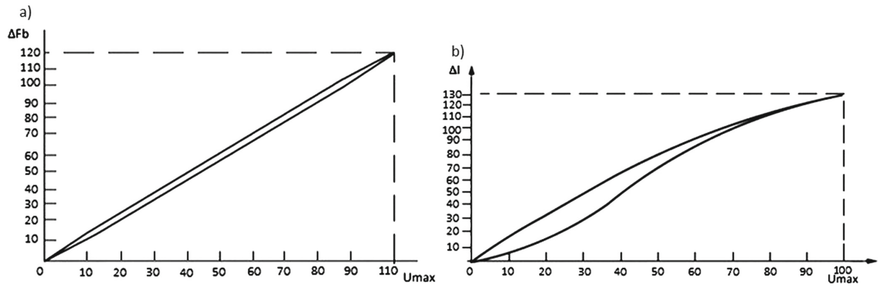

Fig. 4 Dependence of **a** the generated force and of **b** the piezoelement's travel on the voltage

Hysteresis is the property of a physical system not to react instantly to an applied impact, or not to return fully to its original state after such impact. The hysteresis phenomenon must be taken into account when a piezoelectric actuator in used in open-circuit control loops. The dielectric and electromagnetic hysteresis appears in piezoelectric drives under high control voltage and is caused by the behavior of the polarized crystalline structure and molecular effects in piezoceramics [23].

The value of the hysteresis in a piezoelectric actuator is proportional to the control voltage (field strength). The "dip" in the curve of the displacement versus voltage usually starts at 2% (weak signal) and lasts up to 10–15% when a "strong signal" is applied, that is the highest typical value for shear actuators. For example, if the control voltage of a piezoelectric actuator with a stroke of 50 μm is increased by 10%, the equivalent displacement increase is approximately 5 μm. In that case, the position repeatability is still within 1% of the full stroke, or about 1 μm. The smaller displacements are connected with less unreliability. Comparing to typical travel of foils in thrust bearings during their operation, resolution of control system about 1 μm is enough to provide an appropriate range and accuracy of stiffness control in middle- and large-scale microturbines. Diagrams illustrating the hysteresis phenomena in piezoelectric actuators are shown in the Fig. 4. Reduction of the hysteresis influence can be implemented by developing optimal control laws and using closed-loop systems [24–28]. It allows increase the control accuracy in foil bearings for smaller microturbines and increase their operation speed as well.

4 Results of Modeling

Design parameters of a multilayer foil influence a lot on operation of a whole active foil. Its operation mostly depends on mechanical, including strengths and geometrical, characteristics of components of a foil, and characteristics of used piezomaterial.

Modeling was held using the equations above and the following main parameters of a rotor-bearing system: bearing outer diameter is 100 mm, inner diameter is 40 mm, number of foils is 6, rotor mass is 5.5 kg, piezoelectric material is an analogue to CTS-19 with piezoelectric modules (d_{31} d_{33} d_{15}) of (-170 350 400) $\times$ 10^{-12} C/N. The variable parameters are: material of the central base of a multilayer foil, namely the Young's modulus of the material E and the ratio of thicknesses of the central base and of a piezoelectric plate:

$$R_h = \frac{\delta - h_p}{h_p}, \quad (7)$$

where δ is foil thickness, h_p is thickness of piezoelement.

All variations of the parameters above were studied with the range of applied voltage U of 0.100 V DC. Also, all modeling results for foil travel were obtained for free ends of foils under static load equal to the rotor weight, and the weight is distributed on all foils.

Different ratios of thicknesses of the central base and of a piezoelectric plate at constant thickness of a foil δ of 0.9 mm result in its different travel. Combinations of tested parameters are shown in Table 1. The results of calculation are shown in Fig. 5a.

Table 1 Combinations of layers thicknesses of a foil

Foil thickness δ, (mm)	Piezoelement thickness h_p, (mm)	Parameter R_h
0.9	0.48	0.875
0.9	0.45	1
0.9	0.3	2
0.9	0.225	3
0.9	0.15	5

The calculation shows that maximal travel is obtained at minimal thickness of the central base and maximal thickness of a piezoelement plate. The minimum thickness of the central base is limited by limits of its elastic deformation.

Deformation of a multilayer foil also depends on mechanical properties of the material of the central base that can be described by the Young's modulus E. The studied materials were aluminum with E of 70 GPa, copper with E of 110 GPa, and steel with E of 200 GPa. The results of calculation are shown in Fig. 5b. They show that foil's travel range almost does not depend on the material of the central base, so almost any metal that meets other requirements can be used for it.

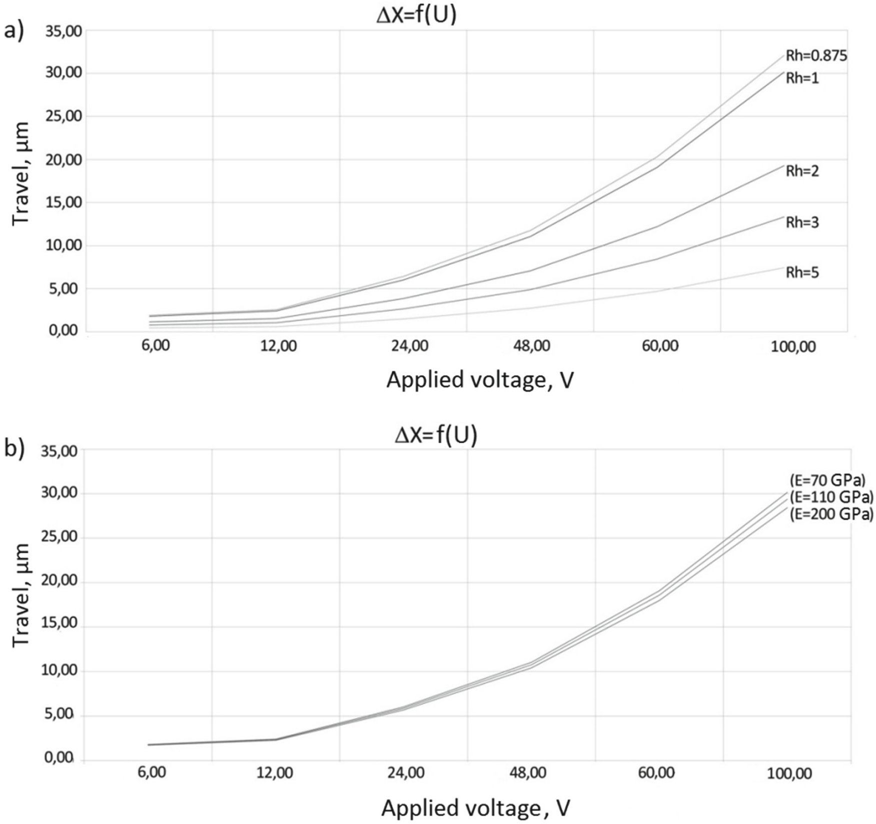

Fig. 5 **a** Foils maximal travel under load depending on applied voltage and full foil and piezodrive thickness ratio; **b** foils maximal travel under load depending on applied voltage and foil material

One of the main effects of using controllable foil bearings is direct controlling of stiffness of a rotor-bearing system caused by its changed shape and the generated force. It also leads to indirect control of damping characteristics, but they are not considered in this article. As the stiffness influences on critical frequencies values in a rotor-bearing system, changing it causes changing the critical frequencies and the rotational speeds at which a resonance phenomenon is observed. Operation at resonance frequency causes extreme loads on bearings and can damage its elements due to high vibrations amplitude. This problem is actual for high-speed flexible shafts of microturbines that usually have several critical frequencies within the operating frequencies range. The results of modeling a rotor-bearing system with active foil bearings and its influence on the system's frequency response is shown in Fig. 6. Applying voltage to piezodrives changes the parameters of stress–strain state of a whole foil, including its stiffness. Direction of changes depends on polarity of applied voltage. In the modeled system, increasing the voltage results in increasing a foil's and, consequently, a whole bearing's stiffness. Changing bearing's stiffness results in shift of critical frequencies of a rotor-bearing system.

Some important points in Fig. 6 during acceleration of a rotor are named with numbers 1–4. After reaching the point 1, the voltage applied to piezoelectric drives in foils was increased from 0 to 60 V. The shifted frequency response leads to shift of the resonance zone and decrease of vibration amplitude. Point 2 is connected with the reverse process in the rotor-bearing system. Points 3 and 4 show the effect similar to points 1 and 2, but for higher rotation frequencies. Such operation is possible for an active thrust foil bearing and cannot be implemented without changing the bearing characteristics in a conventional passive foil thrust bearing.

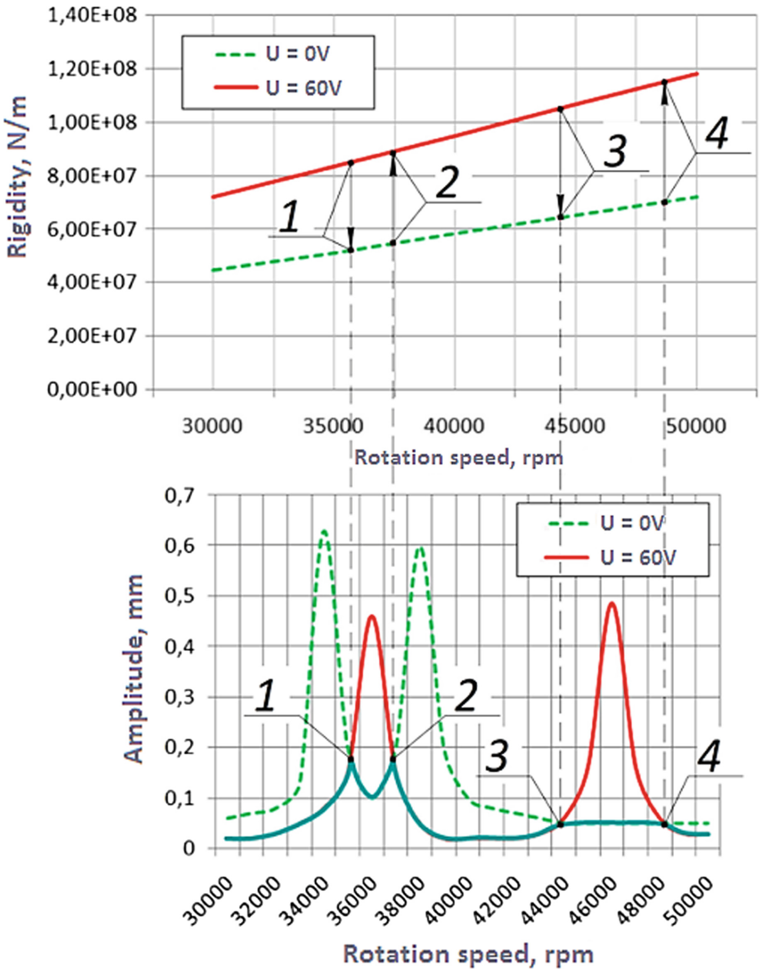

Fig. 6 Rotor-bearing rigidity and frequency response depending on voltage applied to piezoelectric drives

5 Discussion

Applying foil bearings in microturbine power generation sets allows increasing rotation speed and efficiency of power generation. Though, vibrations problem is still actual for such systems. Vibrations can be even more dangerous due to high rotation speed. The modeled operation of a rotor-bearing system during its acceleration to a typical rotation speed shows that control system reduces vibrations amplitude by changing the system's frequency response.

Developing a rotor-bearing system with thrust foil bearings with piezoelectric drives should include several important steps. First of all, the construction of a multilayer foil should be considered in details. The materials and their parameters, including thicknesses of layers, determine the resulting parameters of a bearing. Since the considered approach is relatively new and there are no well-established approaches to design of multilayer foils, some obtained results can help in choosing parameters of a designed bearing. Besides, designing of an active foil bearing should include determining the system's frequency response at various values of voltage applied to piezoelectric drives. The result should be an algorithm of adjusting the voltage that would result in maximal distance of the rotor-bearing system from its resonance frequencies for all rotation frequencies. Also other nonlinear hydrodynamic effects and rotor instabilities can be taken into account in such algorithms. The obtained frequency response of an adjustable rotor-bearing system also should be must be correlated with the planned operating modes of the microturbine plant, especially at the most unstable and dangerous modes, such as starts, stops, changes of load due to different reasons.

Acknowledgements. This work was supported by the Russian Science Foundation, project No. 16-19-00186.

References

1. Hansen CJ, Bower J (2004) An economic evaluation of small-scale distributed electricity generation technologies. Oxford institute for energy studies and department of geography, Oxford University
2. Bauen A, Hawkes A (2004) Decentralised generation—technologies and market perspectives. IEA, Paris
3. Decentralised generation technologies: potentials, success factors and impacts in the liberalized EU energy markets (2002) Fin. Rep., DECENT
4. Ackermann T, Anderson G, Soeder L (2001) Distributed generation: a definition. El Pow Syst Res 57:195–204. https://doi.org/10.1016/s0378-7796(01)00101-8
5. Keyko AV (2010) Formation of predictive technological research in the energy sector. Sys St in the Ener Sect Retrosp of Sc Dir SEI ISEM, Nauka, Novosibirsk, pp 127–146
6. Stennikov VS, Voropai NI (2014) Centralized and distributed generation—not an alternative, but integration. Proceed RAS Energy 1:64–73
7. Khovalova TV (2017) Modeling the effectiveness of the transition to its own generation. Eff Anti-Cris Man 3(102):44–57
8. Bushuev VV, Livinskiy PA (2015) Energy efficient metropolis—Smart City "New Moscow". Energiya Publishing, Moscow

9. Rújula AB (2005) Definitions for distributed generation: a revision. RE&PQJ 1:3
10. European Smart Grid technology platform: Vision and strategy for Europe's networks of the future (2006) European commission, Brussels
11. Nobuo T (1992) Gas Bearing. JP Patent 0,454,309, 21 Feb 1992
12. Prakash Raju GKS, Kumar PA, Rao KS, Aravapalli V (2017) Design and simulation of cantilever based MEMS bimorph piezoelectric energy harvester. Mech Mat Sci Eng J 9:85–90. https://doi.org/10.2412/mmse.16.9.490
13. Sofronov A, Nikiforov V, Klimashin V (2003) Bimorphic piezoelectric elements: actuators and sensors. Compon Technol 30:46–48
14. Nuriev MA et al (2004) On the features of piezoelectricity in polymer compositions with non-uniform polarization. EOM 2:55–58
15. Heinemann B et al (2010) Mechatronics: components, methods, examples: teaching book. SO RAS, Novosibirsk
16. Panichev AE (2008) Piezoceramic actuators: teaching book. Rostov-on-Don
17. Rakotondrabe M, Ivan I (2010), In: IEEE International Conference on Robotics and Automation, May 2010, Anchorage, Alaska, USA, pp 1580–1585
18. Sharapov V (2011) Piezoceramic sensors. Springer Verlag, Heidelberg, Dordrecht, London, New York
19. Peshti YuV (1993) Gas lubrication. MSTU n.a. N.E, Bauman, Moscow
20. Kheshmet Kh, Walowit JA, Pinkus O (1983) Analysis of a gas tape radial bearing. Probl Fric Lub 105(4):124–132
21. Timoshenko SP, Voinovskiy-Kriger S (1966) Plates and shells. Nauka, Moscow
22. Kolkunov NV (1972) Basics of calculating elastic shells. Vysshaya Shkola, Moscow
23. Bobtsov AA, Boikov VI, Bystrov SV, Grigoriev VV (2011) Actuators and systems for micromotion. ITMO, Saint-Petersburg
24. Nekrasov MM, Lavrinenko VV, Bozhko AA (1980) Elements of piezoelectronics and the possibilities of their application in electrical engineering. Electricity 12:51–59
25. Lavrinenko VV, Kartashev IA (1972) Piezoelectric motors. Mashinostroenie, Moscow
26. Dhagupov RG, Erofeev AA (1986) Piezoelectric elements in instrumentation and automation. Mashinostroenie, Leningrad
27. You S, Jin L, Hu J et al (2015) The Danish perspective of energy internet: from service-oriented flexibility trading to integrated design, planning and operation of multiple cross-sectoral energy systems. Zhongguo Dianji Gongcheng Xuebao 35(14):3470–3481
28. Zhang X (2008) A framework for operation and control of smart grids with distributed generation. In: Power and energy society general meeting—conversion and delivery of electrical energy in the 21st century, pp. 1–5. IEEE